



Research Article

## Synthesis of Transition Metal-Nanochitosan Composites Using Ni, Cu, Zn, and Ag Metal Ions and Applications as Antibacterial Agents

Khoirina Dwi Nugrahaningtyas<sup>1,\*</sup>, Eny Kusrini<sup>2,3,4,\*\*</sup>, Salwa Salsabila<sup>1</sup>, Dina Fitriana<sup>1</sup>, Anwar Usman<sup>5</sup>, Triana Kusumaningsih<sup>1</sup>, Sri Juari Santoso<sup>6</sup>

<sup>1</sup>Department of Chemistry, Faculty of Mathematics and Natural Sciences, Sebelas Maret University, Surakarta, 57124 Indonesia

<sup>2</sup>Department of Chemical Engineering, Faculty of Engineering, Universitas Indonesia, Kampus Baru UI, Depok 16424, Indonesia

<sup>3</sup>Research Group of Green Product and Fine Chemical Engineering, Laboratory of Chemical Product Engineering, Department of Chemical Engineering, Universitas Indonesia, Kampus Baru UI, Depok, 16424, Indonesia

<sup>4</sup>Tropical Renewable Energy Research Center, Faculty of Engineering, Universitas Indonesia, Kampus Baru UI, Depok, 16424, Indonesia

<sup>5</sup>Department of Chemistry, Faculty of Science, Universiti Brunei Darussalam, Jalan Tungku Link, Gadong BE1410, Brunei Darussalam

<sup>6</sup>Department of Chemistry, Faculty of Mathematics and Natural Sciences, Universitas Gadjah Mada, Yogyakarta 55281, Indonesia

\*Corresponding author: [khoirnadwi@staff.uns.ac.id](mailto:khoirnadwi@staff.uns.ac.id); Tel.: +62-271-663375; Fax: +62-271-663375

\*\*Corresponding author: [eny.k@ui.ac.id](mailto:eny.k@ui.ac.id); Tel.: +62-21-7863516 Ext. 204

**Abstract:** Nanocomposites are used as antibacterial agents in the pharmacology sector. Therefore, this research aimed to investigate the synthesis, characterization, and antibacterial activity of the transition metal-nanochitosan composites (TM-NCs) using Ni (nickel), Cu (cuprum), Zn (zinc), and Ag (silver) as TM and nanochitosan as the nanomaterial. TM-NCs were synthesized using precipitation method with sodium tripolyphosphate (STPP) as a cross-linking agent. The synthesized products were characterized using X-ray Fluorescence (XRF), X-ray Diffraction (XRD), Fourier Transform Infrared (FTIR), and Scanning Electron Microscopy (SEM) instruments. The metal phase attached to NCs was a metal oxide with irregular particle shapes and various particle sizes. Meanwhile, chitosan and STPP functional groups, namely NH<sub>2</sub> and P-O were bound to the metal to form TM-NCs nanocomposite. The test for antibacterial activity against gram-positive (*Streptococcus pyogenes* ATCC 19615 and *Bacillus cereus* ATCC 10556) and gram-negative (*Escherichia coli* ATCC 11229 and *Klebsiella pneumoniae* ATCC 13883) bacterial strains was carried out using the well-diffusion method. The results showed that Ni-NCs antibacterial activity had the largest inhibition zone compared to the other TM-NCs. Furthermore, Ni-NCs presented the largest inhibitory zone diameter (21.74 mm) towards the gram-positive bacterium *S. pyogenes*.

**Keywords:** Antibacterial; Chitosan; Cross-linking agent; Nanocomposite; Transition metal; Transition metal-nanochitosan

---

This work was supported by the BPPTNBH under the Indonesian Collaboration Research Program (RKI) Scheme C [Decision Letter No. 624/UN27/HK/2022 and Contract No. 872.1/UN27.22/PT.01.03/2022]

<https://doi.org/10.14716/ijtech.v16i1.6969>

Received February 2024; Revised March 2024; Accepted April 2024; Published January 2025

## 1. Introduction

Nanotechnology is a branch of science that studies the application of nanoparticles for various purposes, such as nanocomposites. Nanoscience is a fascinating field since nano-sized composites have high surface reactivity, a greater surface area, and special physicochemical characteristics (Usman et al., 2018) that attract the attention of researchers. Nanoscience is used in various fields, including environmental science (Zamiah et al., 2021; Choi, 2016), biomedicine, biosensors (Supriyono et al., 2023; Wibowo et al., 2021; Hayat et al., 2019; Manikandan et al., 2016; Rezaei et al., 2016), catalysts (Riyadhi et al., 2022), packaging (Haerudin et al., 2010), food processing (Patrulea et al., 2015), antibacterial (Omar et al., 2020), antifungal, and antioxidant (Vieira et al., 2022). Meanwhile, transition metal (TM) nanoparticles have been reported to have various bioactivities, including antibacterial activity. Several research have used biopolymers as ecologically benign stabilizers for metal nanoparticles. Tien and friends stated that silver (Ag) in nanoparticles was more efficient to use as an antibacterial agent than Ag in its ion and bulk form (Kaur et al., 2013; Tien et al., 2009). Cuprum (Cu) nanoparticles were also reported to inhibit the growth of *Escherichia coli* (*E. coli*) and *Klebsiella pneumoniae* (*K. pneumoniae*) bacteria (Syame et al., 2017).

TM nanoparticles tend to agglomerate (Wang et al., 2019), and this tendency is a weakness that can affect their chemical and biological properties. Therefore, modification, including the addition of stabilizers (hydrogels and polymers), is required to control the formation of nanoparticles and dispersion stability during the synthesis of TM nanoproducts. Chitosan (Cs) is a commonly used biopolymer due to its hydroxyl (-OH) and amine (-NH<sub>2</sub>) groups, which can bind to TM ions and lessen TM nanoparticle agglomeration (Kusrini et al., 2021; Chandrasekaran et al., 2020). Chitosan has antibacterial properties (Bashal et al., 2022; Yuan et al., 2016), degrades (Salehi et al., 2016), and is non-toxic, implying that it can increase the bioactivity of TM nanoparticles (Annur et al., 2022). Modification of TM nanoparticles with chitosan polymer as matrix produces nanocomposites. Chitosan nanocomposites (NCs) and their applications have been reported by Usman et al. (2024), Kusrini et al. (2023a; 2023b), and Rosman et al. (2023).

Kusrini and coworkers reported praseodymium-chitosan (Pr-Cs) nanocomposites as adsorbent to remove fluoride ions from aqueous solution (Kusrini et al., 2019). Samarium-chitosan composites (Sm-Cs) were reportedly used in drug delivery systems due to the potential to increase medication (Kusrini et al., 2014). Meanwhile, lead-chitosan (Pd-Cs) nanocomposites can potentially cure cancer cells (Shahriari et al., 2021). Other metal-Cs nanocomposites showed reasonable antibacterial activity against various pathogens (Bharathi et al., 2019; Packirisamy et al., 2019; Bui et al., 2017). Previous research found that nickel oxide-chitosan nanocomposites was used in biomedical applications due to their excellent antibacterial activity against a variety of pathogenic bacteria (Rathore et al., 2021; Mizwari et al., 2020; Das et al., 2018; Rahman et al., 2018).

Metal-Cs are bound through electrostatic interactions between polymer functional groups and nanoparticles, while other interactions occur by ion exchange between metal anions in acid solutions and Cs. Both types of interactions produce metal-Cs composites (Dhanavel et al., 2018; Salehi et al., 2016). The synthesis and application of NCs have been extensively explored by various methods, such as emulsion cross-linking (Riegger et al., 2018), conservation of suspensions (Aloys et al., 2016), reverse micellar extraction (Yang et al., 2010), emulsion-droplet coalescence (Balcerzak et al., 2013), ionic gelation (Usman et al., 2018), and sieving (Yang et al., 2010). However, these methods are complex, relying on organic solvents, surfactants, precipitating agents, and potentially hazardous binding agents such as glutaraldehyde (Aditiya et al., 2015). An alternative material for cross-linking that is safe to use is known as sodium tripolyphosphate (STPP). Chitosan and tripolyphosphate can cross-link using STPP, producing micrometer-sized chitosan (Lee et al., 2001). Exposing chitosan to an acidic environment causes -NH<sub>2</sub> group in its structure to become protonated to -NH<sub>3</sub><sup>+</sup>, converting the chitosan to a polyelectrolyte. The positively charged amino groups of chitosan and the negatively charged counter-ions of STPP will interact ionically when STPP is added as a cross-linking agent, enabling the successful production of chitosan beads. STPP

can interact with chitosan through electrostatic interactions to form a bead structure with better stability, and a shorter time required for formation. Chitosan, which is a crystalline polymer (Suhaimi et al., 2025), will experience a decrease in crystallinity after being cross-linked with  $\text{H}_3\text{P}_3\text{O}_{10}^{2-}$  from STPP. The tripolyphosphate ion from STPP donates a (-OH) group as an electron donor, thereby increasing the number of metal ions bound to the active site. The more ions that are bound, the greater the antibacterial activity. Meanwhile, dispersing metal nanoparticles onto chitosan uses various surfactants such as Tween 20 and 80, sodium dodecyl sulfate, trisodium citrate, and span-20. Among these surfactants, Tween 20 is often used because it can reduce interfacial tension and increase the adhesion of TM nanoparticles to chitosan (Bartmański and Pawłowski, 2021).

NiO nanoparticles synthesized using the coprecipitation method had a high antibacterial effect against gram-negative bacteria *K. pneumoniae* and *P. Vulgaris* (Rahman et al., 2018). The synthesis of Cu/ZnO nanoparticles by the coprecipitation method showed perfect activity against bacteria (Abureesh et al., 2018). ZnO nanoparticles showed good antibacterial activities (Emami-Karvani and Chehrizi, 2011), while nanoparticles of ZnO,  $\text{TiO}_2$ , and  $\text{Ag}_2\text{O}$  combined with chitosan showed increased antibacterial activities (Bui et al., 2017). According to several reported research, synthesis was carried out using reducing agents such as hydrazine hydrate (Peña-Miller et al., 2020), sodium borohydride ( $\text{NaBH}_4$ ) (Dhanavel et al., 2018), and ethylene glycol (Ahmed et al., 2021), which can cause toxicity (Kaur and Kyle, 2022). Therefore, it is necessary to synthesize TM nanoparticles without using toxic reducing agents.

The purpose of this research was to create transition metal-chitosan nanocomposites (TM-NCs) by the co-precipitation method without using reducing agents. Meanwhile, STPP and tween-20 were used as cross-linking and dispersing agents, respectively. The synthesis and characterization of TM-NCs were reported in detail, where TM is transition metal (Nickel (Ni), Cu, Zinc (Zn), or Ag) and NCs is Nano chitosan. The effects of TM in forming TM-NCs towards gram-positive and gram-negative pathogens, including *Streptococcus pyogenes* (*S. pyogenes*), *Bacillus cereus* (*B. cereus*), *E. coli*, and *K. pneumonia*, were evaluated.

## 2. Methods

### 2.1. Materials

The main ingredient in this research was commercial chitosan of pharmaceutical grade (Mr. 501.5 and deacetylation degree of 87.5%). Tween-20, Ni  $(\text{CH}_3\text{COO})_2$ ,  $\text{Cu}_2(\text{CH}_3\text{COO})_4$ , Zn  $(\text{CH}_3\text{CO}_2)_2$ , Ag  $(\text{CH}_3\text{CO}_2)$ , and glacial acetic acid were purchased from Merck (Germany) with pro-analytical quality. Meanwhile, sodium tripolyphosphate was purchased from Sigma Aldrich (USA).

### 2.2. Synthesis of NCs

NCs was synthesized using a precipitation according to the method modified by Dhanavel et al. (2018). A chitosan solution in 2% acetic acid was agitated for 1 hour before being allowed to stand for 24 hours and filtered. Subsequently, Tween-20 was gradually added (Lee et al., 2001), followed by STPP before stirring for 45 minutes. The acidity of the sample was adjusted to the range of 6.5–6.8 by adding 1 M NaOH. The suspension formed was filtered and dried at  $120^\circ\text{C}$  for 3 hours, and the obtained result labeled as NCs.

### 2.3. Synthesis of TMs-NCs

A chitosan solution in 2% acetic acid was agitated for 1 hour before being allowed to stand for 24 hours and filtered. The subsequent phase was the gradual addition of Tween-20 (Lee et al., 2001), followed by 15 wt% nickel acetate metal salt and STPP while stirring for 45 minutes. The sample acidity was adjusted to the range of 6.5–6.8 by adding 1 M NaOH. The suspension formed was filtered and dried at  $120^\circ\text{C}$  for 3 hours and the results labeled as Ni-NCs nanocomposites. The same procedure was repeated for the preparation of Cu, Zn, and Ag to produce Cu-NCs, Zn-NCs, and Ag-NCs nanocomposites.

#### 2.4. Characterization of TMs-NCs

Diffraction analysis was performed using X-ray Diffraction (XRD) (Shimadzu 700 maxima) at a wavelength of 0.154 nm from Cu K $\alpha$  radiation, with a voltage of 40 KV and a current of 50 mA. Data were recorded between 2 theta angles of 10° and 80° with a scanning phase of 2° min<sup>-1</sup> or 0.04°/s. The functional groups of NCs and TM-NCs were investigated using FTIR (Shimadzu Prestige 21) and the morphology was analyzed using Scanning Electron Microscopy (SEM) (Jeol JSM-IT200).

#### 2.5. Antibacterial Investigation

Antimicrobial properties of TM-NCs were determined using the well-diffusion methods (Anitha et al., 2018). Muller Hinton Agar (MHA) was poured into a Petri dish and autoclaved at 121°C for 20 minutes to obtain a solid agar medium. Fresh bacterial cultures were distributed with a sterile cotton swab throughout the dish using a spread plate method. In the next phase, holes were drilled in MHA with a 6 mm cork borer. Each TM-NC and control with a concentration of 15% (w/v) dropped as much as twenty microliters on the hole. The inhibition zone was measured after incubation at 37°C for 24 hours.

### 3. Results and Discussion

#### 3.1. Crystallinity and Phase Composition

The phase composition and crystallinity of TMs-NCs nanocomposite were analyzed using XRD. The results were also used to determine the success of the preparation of TMs-NCs. The characteristic peaks of chitosan (JCPDS data card # 00-039-1894) appeared at 2 $\theta$  of 23.8, 29.9, and 36.3°, which corresponds to basal spacing  $d = (2\ 0\ 1)$ ,  $(1\ 2\ 2)$ , and  $(3\ 1\ 2)$  (Figure 1). The results showed that the diffraction pattern of commercial chitosan was consistent with the characteristics of chitosan reported by previous research (Kaur et al., 2021; Narudin et al., 2020).

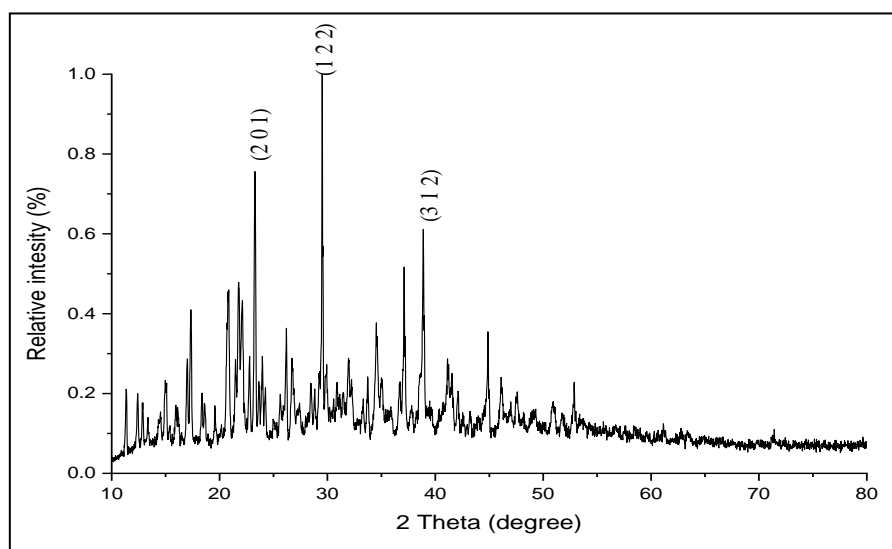


**Figure 1** XRD pattern of commercial chitosan

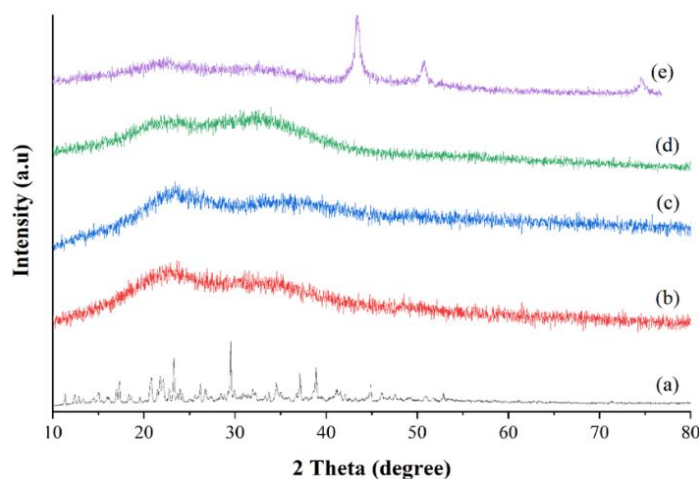
A significant change in the diffraction pattern characterizes the change in chitosan into nano chitosan. Figure 2A shows that the characteristic peak of chitosan disappears and broadband appears at an angle of  $2\theta = 15\text{--}35^\circ$ . The shift in the diffraction pattern shows that chitosan structure shifted from crystalline to amorphous nanoparticles. The results of this research are consistent with the research by Morsy et al. (2019).

Figure 2B-2E shows that the diffraction patterns of TM-NCs samples are similar. This pattern signifies that chitosan nanoparticles are the dominant phase (NCs). Previous research showed that the diffraction pattern of NCs was typical of an amorphous structure (Khoerunnisa et al., 2018).

NCs comprise an extensive network of interpenetrating polymer chains connected by TPP counter ions (Tang et al., 2003). Chitosan nanoparticle chains will disintegrate after cross-linking, resulting in crystallinity degradation.

In this research, TM was proven to be embedded in NCs by comparing the diffraction patterns of TM-NCs and standards using Rietveld refinement with Rietica software. The diffraction patterns of each TMs-NCs sample were compared to standard diffraction patterns from the Cambridge Crystallographic Data Center (CCDC # 1951228) for Cs and the Inorganic Crystal Structure Database (ICSD) for the oxides NiO (#61544), CuO (#61323), ZnO (#52362), and AgO (#605625).

The peaks of Ni-NCs at  $23.59^\circ$  and  $34.56^\circ$  are similar to Cs and Ni pattern characteristics. This peak is close to the standard Cs peak at  $2\theta = 21.84^\circ$  and the standard Ni peak at  $2\theta = 37.30^\circ$ . Cu-NCs peaks at  $23.44^\circ$  and  $36.10^\circ$  were close to the standard Cs peaks at  $2\theta = 21.84^\circ$  and the standard Cu peaks at  $2\theta = 36.71^\circ$ . The peaks of Zn-NCs at  $23.65^\circ$  and  $33.98^\circ$  are close to the peaks of standard Cs, which are at  $2\theta = 21.84^\circ$  and  $2\theta = 34.32^\circ$ , respectively. Ag-NCs had  $2\theta$  peaks at  $22.63^\circ$ ,  $32.60^\circ$ ,  $43.44^\circ$ ,  $50.71^\circ$ , and  $74.59^\circ$ , which were close to Cs standard peak at  $2\theta = 21.84^\circ$ , and Ag standard peak at  $2\theta = 44.3^\circ$  from the face-centered cubic structure of Ag with the Miller index of 200 (Ali et al., 2011).



**Figure 2** XRD patterns of (A) NCs, (B) Ni-NCs, (C) Cu-NCs, (D) Zn-NCs, and (E) Ag-NCs

The diffraction pattern analysis showed that the calculated (-) and experimental (+) data were comparable (observed by a straight green line), showing that the Rietveld refinements are acceptable (see Figures S1- S8). Each TM-NCs data set was compatible with ICSD and CCDC oxide and chitosan standards, with  $R_p/R_{wp}$  values of 6.07 and 7.83, 5.89 and 8.12, 7.25 and 7.37, and 8.82 and 9.48, for Ni-NCs, Cu-NCs, Zn-NCs, and Ag-NCs, respectively (see Table S1).

### 3.2. Functional Group Analysis

The qualitative functional groups of NCs were investigated by comparing the vibrational wavenumbers of Cs and NCs (see Figure 3). Fourier Transform Infrared (FTIR) spectra of chitosan showed a broad absorption at  $3419\text{ cm}^{-1}$ , signifying an overlap in the stretching vibration of OH group with NH group of the amine. The vibrational bands at  $2977$  and  $2941\text{ cm}^{-1}$  correspond to anti-symmetric and symmetric stretching vibrations of C-H, respectively (Thandapani et al., 2017). A vibrational band at  $1579\text{ cm}^{-1}$  represents C=O stretching vibration of amide II, while the bands at  $1548$  and  $1475\text{ cm}^{-1}$  is typical of chitosan, corresponding to  $-\text{NH}_2$  and  $-\text{NH}$  groups, respectively (Shenvi et al., 2014). The band around  $1420\text{ cm}^{-1}$  was assumed to be caused by  $\text{CH}_3$  bending vibration of the acetyl group. The band at  $1242\text{ cm}^{-1}$  corresponds to C-N stretching vibration of the N-acetyl glucosamine group. Meanwhile, the band at  $1073\text{ cm}^{-1}$  corresponds to C-O stretching vibration of  $\text{CH}_2\text{OH}$  group (Thandapani et al., 2017). The band at  $664\text{ cm}^{-1}$  is due to out-of- plane N-H bending vibrations.

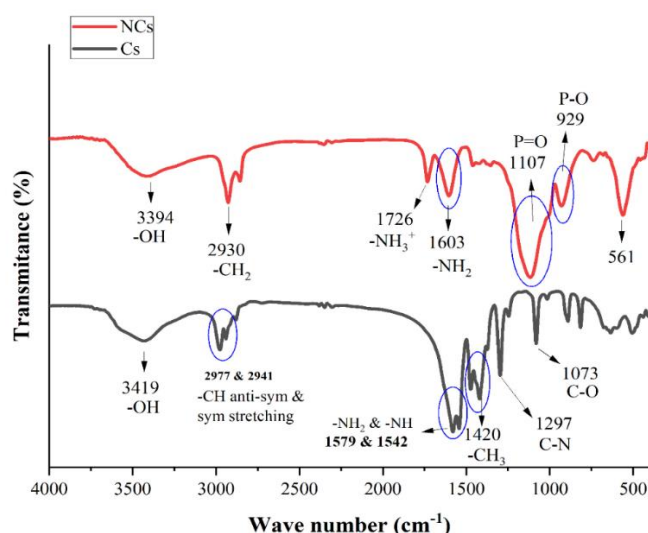


**Figure 3** FTIR spectra of Cs and NCs

The shift and narrowing of the absorption from  $3394\text{ cm}^{-1}$  to  $3419\text{ cm}^{-1}$  showed less hydrogen bonding in NCs due to a more open structure generated by STPP cross-linking (Thandapani et al., 2017). The vibrational bands due to C-H in Cs shifts from  $2977$  and  $2941\text{ cm}^{-1}$  to  $2930$  and  $2855\text{ cm}^{-1}$  in NCs. Furthermore, the vibrations of chitosan  $-\text{NH}_2$  and  $-\text{NH}$  groups appeared at  $1548$  and  $1475\text{ cm}^{-1}$  were observed as a new absorption at  $1603\text{ cm}^{-1}$  in NCs, signifying protonation of the amine group into  $-\text{NH}_3^+$ . This is due to the cross-linking process at acidic pH (Shenvi et al. 2014). The vibrational band at  $1107\text{ cm}^{-1}$  shows the presence of P=O stretching, while the band at  $929\text{ cm}^{-1}$  shows P-O bending, a functional group on the triphosphosphate ion (Thandapani et al., 2017). The appearance of peaks in the specific phosphate group shows that a cross-link between chitosan and STPP has been successfully formed as a result of the ionic interaction between the positive group on chitosan ( $-\text{NH}_3^+$ ) and the negatively charged group  $\text{PO}_3^-$  group or  $\text{PO}_4^{3-}$  group (Yang et al., 2021).

The interaction of TM with Cs in nanocomposites is responsible for the spectral shifts of chitosan functional groups (see Figure 4). The shift towards larger wavenumbers (blue shift) appeared due to stronger bonds in the functional group. Meanwhile, the wavenumber shifts in a smaller direction (redshift) due to the weakened bonds in the functional groups (Nugrahaningtyas et al., 2021).

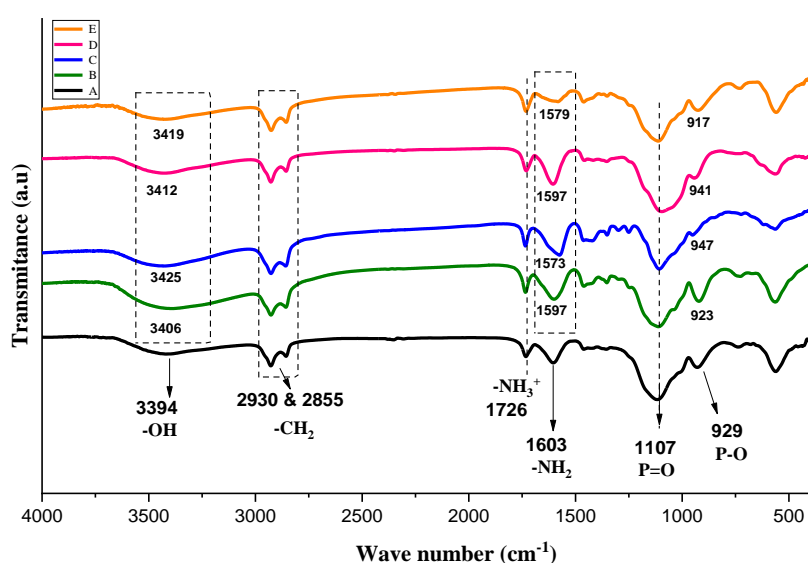


**Figure 4** FTIR spectra of (A) NCs, (B) Ni-NCs, (C) Cu-NCs (D) Zn-NCs, and (E) Ag-NCs

Figure 4 shows that the vibrational band of -CH stretching at 2855-2930  $\text{cm}^{-1}$ , and P=O stretching at 1107  $\text{cm}^{-1}$  is constant. The vibrational band of the protonated amine at 1603  $\text{cm}^{-1}$  and the P-O at 929  $\text{cm}^{-1}$  exhibited a blue shift in all nanocomposites, showing that N-H and P-O bending grew stronger. This modification implies that the metal has been linked to the  $-\text{NH}_3^+$  and P-O groups. The amine group ( $-\text{NH}_2$ ), which is protonated from chitosan, does not directly bind to metal ions but is used to produce chitosan beads. This increases the number of active sites that can bind metal ions. Based on FTIR spectra analysis, the interactions that occurred between TM and NCs can be estimated. The potential interaction between TM and nanochitosan linked with STPP is shown in Figure 5.

### 3.3. Morphology of TM-NCs

Figure 6 shows similarities between the morphology of TM-NCs samples. The morphology was generally irregular, with rough particles that showed agglomeration, and a green color signifying the presence of TM bound to NCs. Energy-dispersive X-ray (EDX) analysis of each sample showed that the metal was present in chitosan. Cu-NC nanocomposites showed a morphology with spherical lumps, which was inconsistent with the results of previous research that the structure of Cu-NCs was cubic (Logpriya et al., 2018). For example, the results of EDX analysis showed that Ni-NCs contained 53.11% C elements, 18.86% O elements, and 7.45% Ni elements. EDX spectra analysis showed that Cu-NCs comprised 63.71% C elements, 12.01% O elements, and 12.93% Cu elements. Meanwhile, the EDX of Zn-NCs showed the presence of C, O, and Zn elements of 46.83%, 18.89%, and 18.66%, respectively. Ag-NCs contain 56.27% C, 15.46% O, and 10.14% Ag elements.

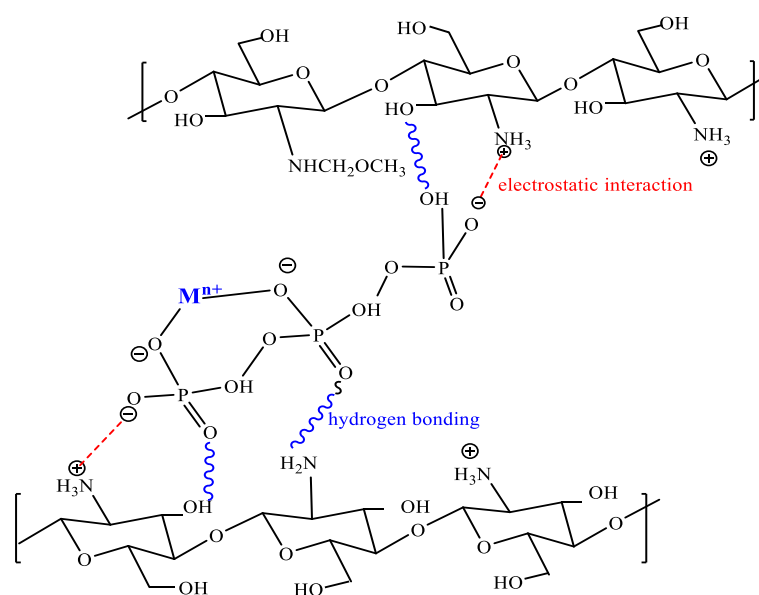


**Figure 5** Proposed scheme of TM bonding with NCs linked STPP

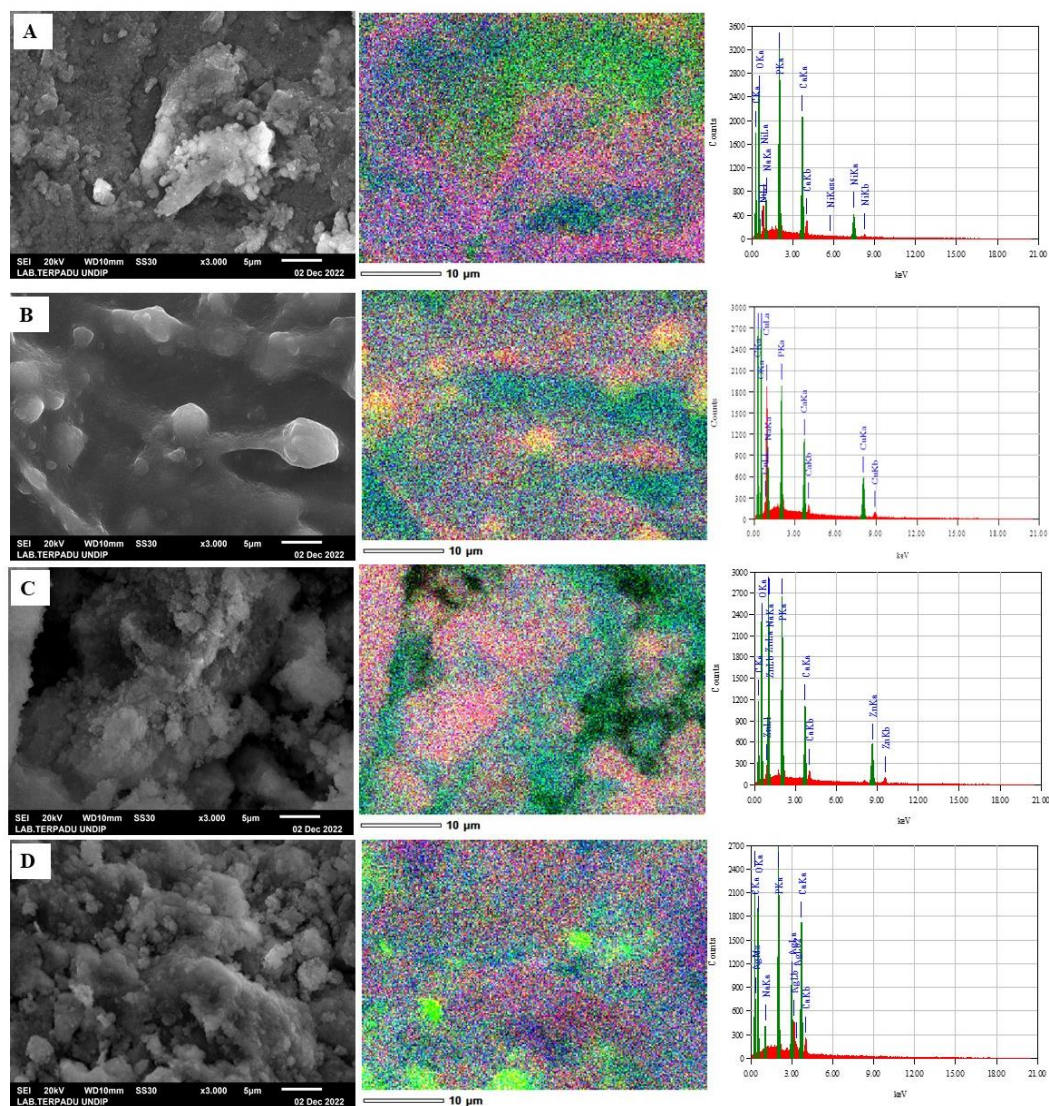


**Figure 6** Morphology and mapping element of (A). Ni-NCs, (B) Cu-NCs, (C). Zn-NCs, and (D) Ag-NCs

### 3.4. Antibacterial activities

This research showed the role of TM role in increasing antibacterial activity of chitosan (Figures 7 and 8). However, this contribution was not observed in the gram-positive pathogens *S. pyogenes* ATCC 19615 and *B. cereus* ATCC 10556. The enormous increase in gram-negative antibacterial *E. coli* ATCC 11229 and *K. pneumoniae* ATCC 13883 from NCs after metal addition shows the significant role of TM. [Adewuyi et al., \(2011\)](#) found that adding TM nanoparticles to chitosan increased acidity. Metal ions bound to chitosan enhanced the electrophilic properties of NCs, while chelated metal ions bound to chitosan increased the positive charge density of chitosan. Furthermore, the polycationic amines interacted strongly with the negatively charged bacterial cell surface due to increased charge density. This occurrence is critical for inhibiting bacterial growth ([Adewuyi et al., 2011](#)).

Previous research found that the more valence electrons and the smaller the radius of the metal ion, the stronger the interaction with chitosan ([Adewuyi et al., 2011](#)). However, due to the most stable electron configuration of Cu, the bond with chitosan weakens, as does its ability to inhibit bacterial growth. This research also discovered that Ni-NCs had the largest inhibitory zone diameter for *S. pyogenes*, measuring 21.74 mm.



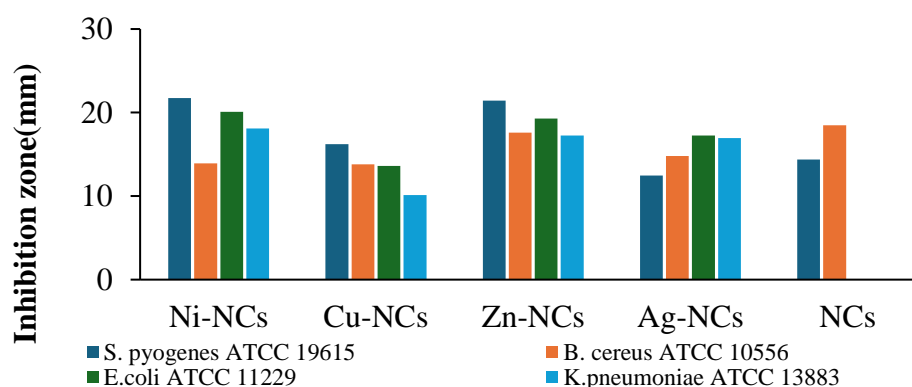


**Figure 7** A comparison of antibacterial activities between Ni-NCs, Cu-NCs, Zn-NCs, Ag-NCs, and N-NCs against *S. pyogenes*, *B. cereus*, *E. coli*, and *K. pneumoniae*

Antibacterial activity is classified into five types. An inhibition diameter of a material less than 5 mm is classified as not having antibacterial properties. Antibacterial power is classified as insignificant in an inhibition zone of 9-12 mm, 13-15 mm weak, 16-18 mm is good, and greater than 18 mm is considered very strong (Hameed, 2014). In this research, Ni-NCs exhibited powerful antibacterial properties against gram-positive bacteria. Ni-NCs had an inhibitory zone of 21.74 mm against the gram-positive bacterium *S. pyogenes*. Cu-NCs had weak antibacterial properties due to the diameter of less than 15 mm, except for the inhibitory diameter of *S. pyogenes*. Antibacterial activities of Ni-NCs, Zn-NCs, and Ag-NCs nanocomposites were comparable to the Gold (Au) metal-based antibacterial material (Sathiyaraj et al., 2021), terbium sulfide nanocomposites capped with chitosan (CS-Tb<sub>2</sub>S<sub>3</sub> NCs) (Kusrini et al., 2023a) and zinc sulfide capped with chitosan (CS-ZnS nanocomposites) (Kusrini et al., 2023b). Both CS-Tb<sub>2</sub>S<sub>3</sub> NCs and CS-ZnS NCs have antibacterial activities against *Staphylococcus aureus* (Kusrini et al., 2023a; 2023b). The antifungal activities of nano- and micro particles of Fe<sub>3</sub>O<sub>4</sub> CS/Sm/Ranitidine composites against *Aspergillus niger* have also been recently reported by Kusrini et al. (2025). The Fe<sub>3</sub>O<sub>4</sub> CS/Sm/Ranitidine composites with a concentration of 1000 µg/mL showed an inhibition zone of the fungal strain in the range from 16.33 mm to 18.33 mm, highlighting their strong antifungal activities.

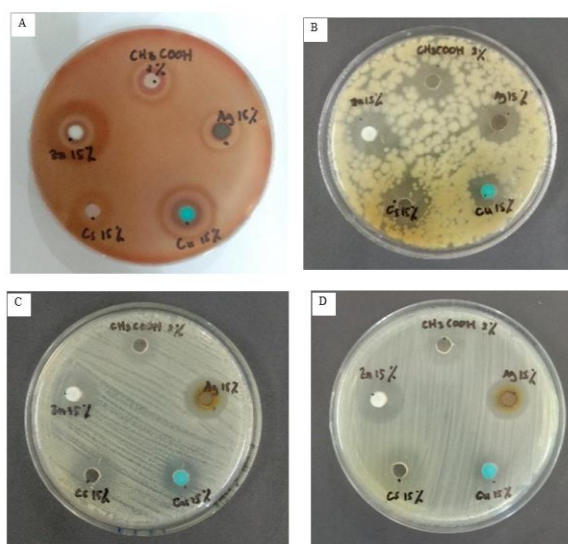


**Figure 8** Antibacterial inhibition image of negative control, NCs, Ni-NCs, Cu-NCs, Zn-NCs, and Ag-NCs against (A) *S. pyogenes*, (B) *B. caerus*, (C) *E. coli*, and (D) *K. pneumonia* in vitro

TM-NCs have antibacterial activity due to their ability to interact with bacterial cell membranes. This interaction inhibits DNA replication, cell division, cell structure, and cell respiration,

increasing membrane permeability. TM-NCs interfere, causing the bacterial cell surface to expand and destroy membrane integrity, leading to cell death (Wang et al., 2020; Hosseinnejad and Jafari, 2016). According to previous research (Mirbagheri et al., 2024; Ke et al., 2021; Li and Zhuang, 2020), the mechanism of antibacterial action of TM-NCs can be divided into several phases. First, electrostatic interactions between cationic amine groups in TM-NCs and negatively charged bacterial cell walls increase membrane permeability and intracellular compound release. In the second phase, TM nanoparticles diffuse into the cell and form a hole, allowing the bacterial membrane to leak and eventually leads to cell death. Another possible mechanism is chitosan coating the bacterial surface, preventing nutrients and oxygen from entering the cell.

#### 4. Conclusions

In conclusion, TM-NCs were successfully synthesized as antibacterial agents without a reduction phase. The results showed that TM caused no structural damage to the host material (chitosan). Furthermore, the metals were used as the oxide phase and distributed on the surface of chitosan. The interaction between TM and nanochitosan was through the protonated  $\text{NH}_2$  and P-O functional groups of chitosan with irregular shapes and sizes. It was observed that the modification and addition of metals to these composites enhanced antibacterial activity of chitosan. Ni-NCs had the strongest antibacterial properties with an inhibitory zone of 21.74 mm against the gram-positive bacterium *S. pyogenes*. It was also found that antibacterial properties of TM were closely related to the periodic table of elements, with antibacterial properties decreasing from left to right.

#### Acknowledgements

The authors are grateful to Universitas Sebelas Maret for financial support for the payment of Article Processing Charge (APC) of this article.

#### Author Contributions

KDN – conceptualization, supervision and analysis; EK – Analysis, writing & review; SS – Experiment & Investigation; DF -Investigation & characterization; AU- Analysis, Editing & review; TK - Formal analysis; SJS – Review.

#### Conflict of Interest

The authors declare no conflicts of interest.

#### References

- Abureesh, MA, Oladipo, AA, Mizwari, ZM & Berksel, E 2018, 'Engineered mixed oxide-based polymeric composites for enhanced antimicrobial activity and sustained release of antiretroviral drug', *International Journal of Biological Macromolecules*, vol. 116, pp. 417-425, <https://doi.org/10.1016/j.ijbiomac.2018.05.065>
- Adewuyi, S, Kareem, KT, Atayese, AO, Amolegbe, SA & Akinremi, CA 2011, 'Chitosan-cobalt(II) and nickel(II) chelates as antibacterial agents', *International Journal of Biological Macromolecules*, vol. 48, no. 2, pp. 301-303, <https://doi.org/10.1016/j.ijbiomac.2010.12.004>
- Aditiya, HB, Sing, KP, Hanif, M & Mahlia, TMI 2015, 'Effect of acid pretreatment on enzymatic hydrolysis in bioethanol production from rice straw', *International Journal of Technology*, vol. 6, no. 1, pp. 3-10 <https://doi.org/10.14716/ijtech.v6i1.784>
- Ahmed, AAA, Al-Mushki, AAA, Al-Asbahi, BA, Abdulwahab, AM, Abduljalil, JMA, Saad, FAA, Qaid, SMH, Ghaithan, HM, Farooq, WA & Omar, AEH 2021, 'Effect of ethylene glycol concentration on the structural and optical properties of multimetal oxide CdO–NiO–Fe<sub>2</sub>O<sub>3</sub> nanocomposites for antibacterial activity', *Journal of Physics and Chemistry of Solids*, vol 155, article 110113, <https://doi.org/10.1016/j.jpccs.2021.110113>
- Ali, SW, Rajendran, S & Joshi, M 2011, 'Synthesis and characterization of chitosan and silver loaded chitosan nanoparticles for bioactive polyester', *Carbohydrate Polymers*, vol. 83, no. 2, pp. 438-446, <https://doi.org/10.1016/j.carbpol.2010.08.004>

Aloys, H, Korma, SA, Alice Tuyishime, M, Chantal, N, Ali, AH, Abed, SM & Ildephonse, H 2016, 'Microencapsulation by complex coacervation: methods, techniques, benefits, and applications-a review', *American Journal of Food Science and Nutrition Research*, vol. 3, no. 6, pp. 188-192, viewed 23 August 2022, ([https://www.researchgate.net/publication/326186301\\_Microencapsulation\\_by\\_Complex\\_Coacervation\\_Methods\\_Techniques\\_Benefits\\_and\\_Applications\\_-\\_A\\_Review](https://www.researchgate.net/publication/326186301_Microencapsulation_by_Complex_Coacervation_Methods_Techniques_Benefits_and_Applications_-_A_Review))

Anitha, S, Suganya, M, Prabha, D, Srivind, J, Balamurugan, S & Balu, AR 2018, 'Synthesis and characterization of NiO-CdO composite materials towards photoconductive and antibacterial applications', vol. 211, pp. 88-96, <https://doi.org/10.1016/j.matchemphys.2018.01.048>

Annur, D, Bayu, F, Supriadi, S & Suharno, B 2022, 'Transdisciplinary research and education center for green technologies', *EVERGREEN Joint Journal of Novel Carbon Resource Sciences & Green Asia Strategy*, vol. 9, no. 1, pp. 109-114, doi: 10.5109/4774222.

Balcerzak, J, Kucharska, M & Gruchala, B 2013, 'Preparation of micro and nanostructures of chitosan by ultrasonic coalescence of W/O emulsions', *Progress on Chemistry and Application of Chitin and its Derivatives*, vol. 18, pp. 13-20

Bartmański, MB & Pawłowski, Ł 2021, 'Properties of chitosan/CuNPs coatings electrophoretically deposited on TiO<sub>2</sub> nanotubular oxide layer of Ti13Zr13Nb alloy', *Materials Letters*, vol. 308, article 130982, <https://doi.org/10.1016/j.matlet.2021.130982>

Bashal, AH, Riyadh, SM, Alharbi, W, Alharbi, KH, Farghaly, TA & Khalil, KD 2022, 'Bio-based (chitosan-ZnO) nanocomposite: synthesis, characterization, and its use as recyclable, ecofriendly biocatalyst for synthesis of thiazoles tethered azo groups', *Polymers*, vol. 14, no. 3, p. 386, <https://doi.org/10.3390/polym14030386>

Bharathi, D, Ranjithkumar, R, Vasantharaj, S, Chandarshekar, B & Bhuvaneshwari, V 2019, 'Synthesis and characterization of chitosan/iron oxide nanocomposite for biomedical applications', *International Journal of Biological Macromolecules*, vol. 132, pp. 880-887, <https://doi.org/10.1016/j.ijbiomac.2019.03.233>

Bui, VKH, Park, D & Lee, YC 2017, 'Chitosan combined with ZnO, TiO<sub>2</sub> and Ag Nanoparticles for antimicrobial wound healing applications: a mini review of the research trends', *Polymers*, vol. 9, no. 1, article 21, <https://doi.org/10.3390/polym9010021>

Chandrasekaran, M, Kim, KD & Chun, SC 2020, 'Antibacterial activity of chitosan nanoparticles: a review', *Processes*, vol. 8, article 1173, <https://doi.org/10.3390/pr8091173>

Choi, SK 2016, 'Mechanistic basis of light induced cytotoxicity of photoactive nanomaterials', *NanoImpact*, vol. 3-4, pp. 81-89, <https://doi.org/10.1016/j.impact.2016.09.001>

Das, B, Moumita, S, Ghosh, S, Khan, MI, Indira, D, Jayabalan, R, Tripathy, SK, Mishra, A & Balasubramanian, P 2018, 'Biosynthesis of magnesium oxide (MgO) nanoflakes by using leaf extract of Bauhinia purpurea and evaluation of its antibacterial property against Staphylococcus aureus', *Materials Science and Engineering: C*, vol. 91, pp. 436-444, <https://doi.org/10.1016/j.msec.2018.05.059>

Dhanavel, S, Manivannan, N, Mathivanan, N, Gupta, VK, Narayanan, V & Stephen, A 2018, 'Preparation and characterization of cross-linked chitosan/palladium nanocomposites for catalytic and antibacterial activity', *Journal of Molecular Liquids*, vol. 257, pp. 32-41, Viewed 23 August 2022, (<https://linkinghub.elsevier.com/retrieve/pii/S0167732218300928>)

Emami-Karvani, Z & Chehrizi, P 2011, 'Antibacterial activity of ZnO nanoparticle on gram-positive and gram-negative bacteria', *African Journal of Microbiology Research*, vol. 5, no. 12, pp. 1368-1373, doi: 10.5897/AJMR10.159

Haerudin, H, Pramono, AW, Kusuma, DS, Jenie, A, Voelcker, NH & Gibson, C 2010, 'Preparation and characterization of chitosan/montmorillonite (MMT) nanocomposite systems', *International Journal of Technology*, vol. 1, no. 1, pp. 65-73, <https://doi.org/10.14716/ijtech.v1i1.33>

Hameed, S 2014, 'Antibacterial and antifungal activities of the crude extracts from the stem of Chenopodium ambrosioides Linn, an indigenous medicinal plant', *African Journal of Pharmacy and Pharmacology*, vol. 8, no. 8, pp. 231-234, <https://doi.org/10.5897/AJPP2014.4010>

Hayat, M, Saepudin, E, Einaga, Y & Ivandini, TA, 2019 'Cds nanoparticle-based biosensor development for aflatoxin determination', *International Journal of Technology*, vol. 10, no. 4, pp. 787-797, <https://doi.org/10.14716/ijtech.v10i4.2407>

Hosseinnejad, M & Jafari, M 2016, 'Evaluation of different factors affecting antimicrobial properties of chitosan', *International Journal of Biological Macromolecules*, vol. 85, pp. 467-475, <https://doi.org/10.1016/j.ijbiomac.2016.01.022>

Kaur, J & Kyle, PB 2022 'Ethylene glycol toxicity', *In: Toxicology Cases for the Clinical and Forensic Laboratory*, pp. 51-54

Kaur, K, Sa' Paiva, S, Caffrey, D, Cavanagh, BL & Murphy, CM 2021, 'Injectable chitosan/collagen hydrogels nano-engineered with functionalized single wall carbon nanotubes for minimally invasive applications in bone', *Materials Science and Engineering: C*, vol. 128, article 112340, <https://doi.org/10.1016/j.msec.2021.112340>

Kaur, P, Choudhary, A & Thakur, R 2013, 'Synthesis of chitosan-silver nanocomposites and their antibacterial activity', *International Journal of Scientific & Engineering Research*, vol. 4, no. 4, article 869, Viewed 16 March 2024 ([https://www.researchgate.net/publication/273455396\\_Synthesis\\_of\\_Chitosan-silver\\_nanocomposites\\_and\\_their\\_antibacterial\\_activity](https://www.researchgate.net/publication/273455396_Synthesis_of_Chitosan-silver_nanocomposites_and_their_antibacterial_activity))

Ke, C.-L, Deng, F.-S, Chuang, C.-Y, Lin, C.-H & Bardosova, M 2021, 'Antimicrobial Actions and Applications of Chitosan', *Polymers*, vol. 13, no. 6, article 904, <https://doi.org/10.3390/polym13060904>

Khoerunnisa, F, Hendrawan, Primastari, DR & Agiawati, R 2018, 'Effect of MWCNT filler on properties and flux of chitosan/ PEG based nanocomposites membranes', *MATEC Web of Conferences*, vol. 156, pp. 1-6, <https://doi.org/10.1051/mateconf/201815604001>

Kusrini, E, Arbianti, R, Sofyan N, Abdullah, MAA & Andriani, F 2014, Modification of chitosan by using samarium for potential use in drug delivery system', *Spectrochimica Acta Part A: Molecular and Biomolecular Spectroscopy*, vol. 120, pp. 77-83, <https://doi.org/10.1016/j.saa.2013.09.132>

Kusrini, E, Ayuningtyas, K, Mawarni, DP, Wilson, LD, Sufyan, M, Rahman, A, Prasetyanto, YEA & Usman, A 2021, 'Micro-structured materials for the removal of heavy metals using a natural polymer composite', *International Journal of Technology*, vol. 12, no. 2, pp. 275-286, <https://doi.org/10.14716/ijtech.v12i2.4578>

Kusrini, E, Irma Safira, A, Usman, A, Prasetyanto, EA, Dwi Nugrahaningtyas, K, Santosa, SJ & Wilson, LD, 2023a, 'Nanocomposites of terbium sulfide nanoparticles with a chitosan capping agent for antibacterial applications', *Journal Composite Science*, vol. 7, no. 1, article 39, <https://doi.org/10.3390/jcs7010039>

Kusrini, E, Nuzula, K, Usman, A, Wilson, LD, Gunawan, C & Prasetyo, AB 2025, 'Enhanced Cytotoxicity and Antifungal Effects of Iron-Oxide Chitosan/Samarium/Ranitidine Microparticles', *Sains Malaysiana*, vol. 54(1), pp. 3675-3688, <http://doi.org/10.17576/jsm-2025-5401-17>

Kusrini, E, Paramesti, SN, Zulys, A, Daud, NZA, Usman, A, Wilson, LD & Sofyan, N 2019, 'Kinetics, isotherm, thermodynamic and bioperformance of defluoridation of water using praseodymium-modified chitosan', *Journal of Environmental Chemical Engineering*, vol. 7, no. 6, article 103498, <https://doi.org/10.1016/j.jece.2019.103498>

Kusrini, E, Wilson, LD, Padmosoedarso, KM, Mawarni, DP, Sufyan, M & Usman, A 2023b, 'Synthesis of chitosan capped zinc sulphide nanoparticle composites as an antibacterial agent for liquid handwash disinfectant applications', *Journal Composite Science*, vol. 7, no. 2, article 52, <https://doi.org/10.3390/jcs7020052>

Lee, ST, Mi, FL, Shen, YJ & Shyu, SS 2001, 'Equilibrium and kinetic studies of copper(II) ion uptake by chitosan-tripolyphosphate chelating resin', *Polymer*, vol. 42, no. 5, pp. 1879-1892, [https://doi.org/10.1016/S0032-3861\(00\)00402-X](https://doi.org/10.1016/S0032-3861(00)00402-X)

Li, J & Zhuang, S 2020 'Antibacterial activity of chitosan and its derivatives and their interaction mechanism with bacteria: Current state and perspectives', *European Polymer Journal*, vol. 138, p. 109984, <https://doi.org/10.1016/j.eurpolymj.2020.109984>

Logpriya, S, Bhuvaneshwari, V, Vaidehi, D, SenthilKumar, RP, Nithya Malar, RS, Pavithra Sheetal, B, Amsaveni, R & Kalaiselvi, M 2018, 'Preparation and characterization of ascorbic acid-mediated chitosan-copper oxide nanocomposite for anti-microbial, sporicidal and biofilm-inhibitory activity', *Journal of Nanostructure in Chemistry*, vol. 8, no. 3, pp. 301-309, doi: 10.1007/S40097-018-0273-6/FIGURES/10

Manikandan, V, Velmurugan, P, Park, JH, Lovanh, N, Seo, SK, Jayanthi, P, Park, YJ, Cho, M & Oh, B-T 2016, 'Synthesis and antimicrobial activity of palladium nanoparticles from *Prunus × yedoensis* leaf extract', *Materials Letters*, vol. 185, pp. 335-338, <https://doi.org/10.1016/j.matlet.2016.08.120>

Mirbagheri, VS, Alishahi, A, Ahmadian, G, Hamidreza, S, Petroudi, H, Ojagh, SM, & Romanazzi, G 2024, 'Toward understanding the antibacterial mechanism of chitosan: Experimental approach and in silico analysis', *Food Hydrocolloids*, vol. 147, article 109382, <https://doi.org/10.1016/j.foodhyd.2023.109382>

Mizwari, ZM, Oladipo, AA & Yilmaz, E 2020, 'Chitosan/metal oxide nanocomposites: synthesis, characterization, and antibacterial activity', *International Journal of Polymeric Materials and Polymeric Biomaterials*, vol. 70, no. 6, pp. 383-391, <https://doi.org/10.1080/00914037.2020.1725753>

Morsy, M, Mostafa, K, Amyr, H, El-Ebissy, A, Salah, A & Youssef, M 2019, 'Synthesis and characterization of freeze dryer chitosan nano particles as multi functional eco-friendly finish for fabricating easy care and antibacterial cotton textiles', *Egyptian Journal of Chemistry*, vol. 62, no. 7, pp. 1277-1293, doi: 10.21608/ejchem.2019.6995.1583

Narudin, NAH, Abdul Hanif Mahadi, AH, Kusriani, E & Usman, A 2020, 'Chitin, chitosan, and submicron-sized chitosan particles prepared from scylla serrata shells', *Materials International*, vol. 2, no. 2, pp. 139-149, <https://doi.org/10.33263/Materials22.139149>

Nugrahaningtyas, KD, Heraldry, E, Hidayat, Y & Kartini, I 2021, 'Effect of synthesis and activation methods on the character of CoMo/ultrastable Y-zeolite catalysts', *Open Chemistry*, vol. 19, no. 1, pp. 745-754, <https://doi.org/10.1515/chem-2021-0064>

Omar, MS, Sanif, MNMNM, Ali, NHSO, Hamid, MHSA, Taha, H, Mahadi, AH, Soon, YW, Ngaini, Z, Rosli, MYH & Usman, A 2020, Synthesis of schiff base encapsulated ZnS nanoparticles: characterization and antibacterial screening, *International Journal of Technology*, vol. 11, no. 7, pp. 1309-1318, <https://doi.org/10.14716/ijtech.v11i7.4486>

Packirisamy, RG, Govindasamy, C, Sanmugam, A, Karuppasamy, K, Kim, HS & Vikraman, D,(2019), 'Synthesis and antibacterial properties of novel ZnMn2O4-chitosan nanocomposites', *Nanomaterials*, vol. 9, no. 11, article 1589, <https://doi.org/10.3390/nano9111589>

Patrulea, V, Ostafe, V, Borchard, G & Jordan, O 2015, 'Chitosan as a starting material for wound healing applications', *European Journal of Pharmaceutics and Biopharmaceutics*, vol. 97, pp. 417-426, <https://doi.org/10.1016/j.ejpb.2015.08.004>

Peña-Miller, R, Alberto, J, Cervantes, G, Naskar, A, Lee, S & Kim, K-S 2020, 'Easy one-pot low-temperature synthesized Ag-ZnO nanoparticles and their activity against clinical isolates of methicillin-resistant staphylococcus aureus', *Frontiers in bioengineering and biotechnology*, vol. 8, article 00216, <https://doi.org/10.3389/fbioe.2020.00216>

Rahman, MA, Radhakrishnan, R & Gopalakrishnan, R 2018, 'Structural, optical, magnetic and antibacterial properties of Nd doped NiO nanoparticles prepared by co-precipitation method', *Journal of Alloys and Compounds*, vol. 742, pp. 421-429, <https://doi.org/10.1016/j.jallcom.2018.01.298>

Rathore, BS, Chauhan, NPS, Jadoun, S, Ameta, SC & Ameta, R 2021, 'Synthesis and characterization of chitosan-polyaniline-nickel(II) oxide nanocomposite', *Journal of Molecular Structure*, vol. 1242, article 130750, <https://doi.org/10.1016/j.molstruc.2021.130750>

Rezaei, B, Shams-Ghahfarokhi, L, Havakeshian, E & Ensafi, AA 2016, 'An electrochemical biosensor based on nanoporous stainless steel modified by gold and palladium nanoparticles for simultaneous determination of levodopa and uric acid', *Talanta*, vol. 158, pp. 42-50, <https://doi.org/10.1016/j.talanta.2016.04.061>

Riegger, BR, Bäurer, B, Mirzayeva, A, Tovar, GEM & Bach, M 2018, A systematic approach of chitosan nanoparticle preparation via emulsion cross-linking as potential adsorbent in wastewater treatment', *Carbohydrate Polymers*, vol. 180, pp. 46-54, <https://doi.org/10.1016/j.carbpol.2017.10.002>

Riyadhi, A, Yulizar, Y & Susanto, BH 2022, 'Catalytic conversion of beef tallow to biofuels using MgO nanoparticles green synthesized by zingiber officinale roscoe rhizome extract', *International Journal of Technology*, vol. 13, no. 4, pp. 900-911, <https://doi.org/10.14716/ijtech.v13i4.4821>

Rosman, N'A, Asrahwi, MA, Narudin, NAH, Mohd Sahid, MS, Dewi, R, Shamsuddin N, Roil Bilad, M, Kusriani, E, Hobley, J & Usman, A 2023, Chapter 7: Chitin and Chitosan: Isolation, Deacetylation, and Prospective Biomedical, Cosmetic, and Food Applications, *In: Advanced Materials towards Energy Sustainability*, pp. 129-150, <https://doi.org/10.1201/9781003367819>

Salehi, E, Daraei, P & Arabi Shamsabadi, A 2016, A review on chitosan-based adsorptive membranes', *Carbohydrate Polymers*, vol. 152, pp. 419-432, <https://doi.org/10.1016/j.carbpol.2016.07.033>

Sathiyaraj, S, Suriyakala, G, Dhanesh Gandhi, A, Babujanarthanam, R, Almaary, KS, Chen, TW & Kaviyarasu, K 2021, Biosynthesis, characterization, and antibacterial activity of gold nanoparticles, *Journal of Infection and Public Health*, vol. 14, no. 12, pp. 1842-1847, <https://doi.org/10.1016/j.jiph.2021.10.007>

Shahriari, M, Sedigh, MA, Mahdavian, Y, Mahdigholizad, S, Pirhayati, M, Karmakar, B & Veisi, H 2021, In situ supported Pd NPs on biodegradable chitosan/agarose modified magnetic nanoparticles as an effective catalyst for the ultrasound assisted oxidation of alcohols and activities against human breast cancer, *International Journal of Biological Macromolecules*, vol. 172, pp. 55-65, <https://doi.org/10.1016/j.ijbiomac.2021.01.037>

Shenvi, S, Ismail, AF & Isloor, AM 2014, Preparation and characterization study of PPEES/chitosan composite membrane cross-linked with tripolyphosphate, *Desalination*, vol. 344, pp. 90-96, <https://doi.org/10.1016/j.desal.2014.02.026>

Suhaimi, NAA, Nur Batrisyia Amirul, NB, Alessandra Anne Hasman, AA, Shahri, NNM, Roslan, NN, Lau, HLH, Kong, CPY, Kusriani, E & Usman, A 2025, 'Insights into depolymerization of chitosan using acid hydrolysis, direct photolysis, and photocatalysis: A review', *Results in Chemistry*, vol. 13, pp. 102044, <https://doi.org/10.1016/j.rechem.2025.102044>

Supriyono, Kartikowati, CW, Poerwadi, B, Wulandari, C, Hikma, LLF, Azzahra, A, Ghanyysyafira, K & Pinastika, HL 2023, 'The Formation Process of Hydroxyapatite Nanoparticles by Electrolysis and Their Physical Characteristics', *International Journal of Technology*, vol. 14, no. 2, pp. 330–338, <https://doi.org/10.14716/ijtech.v14i2.4452>

Syame, SM, Mohamed, WS, Mahmoud, RK & Omara, ST 2017, 'Synthesis of copper-chitosan nanocomposites and their applications in treatment of local pathogenic isolates bacteria', *Oriental Journal of Chemistry, Oriental Scientific Publishing Company*, vol. 33, no. 6, pp. 2959–2969, <http://dx.doi.org/10.13005/ojc/330632>

Tang, ESK, Huang, M & Lim, LY 2003, 'Ultrasonication of chitosan and chitosan nanoparticles', *International Journal of Pharmaceutics*, vol. 265, no. (1–2), pp. 103–114, [https://doi.org/10.1016/S0378-5173\(03\)00408-3](https://doi.org/10.1016/S0378-5173(03)00408-3)

Thandapani, G, Supriya Prasad, P, Sudha, PN & Sukumaran, A 2017, 'Size optimization and in vitro biocompatibility studies of chitosan nanoparticles', *International Journal of Biological Macromolecules*, vol. 104, pp. 1794–1806, <https://doi.org/10.1016/j.ijbiomac.2017.08.057>

Tien, DC, Tseng, KH, Liao, CY & Tsung, TT 2009, 'Identification and quantification of ionic silver from colloidal silver prepared by electric spark discharge system and its antimicrobial potency study', *Journal of Alloys and Compounds*, vol. 473, no. 1–2, pp. 298–302, <https://doi.org/10.1016/j.jallcom.2008.05.063>

Usman, A, Kusri, E, Widianoro, AB, Hardiya, E, Abdullah, NA & Yulizar, Y 2018, 'Fabrication of chitosan nanoparticles containing samarium ion potentially applicable for fluorescence detection and energy transfer', *International Journal of Technology*, vol. 9, no. 6, pp. 1112–1120, <https://doi.org/10.14716/ijtech.v9i6.2576>

Usman, A, Kusri, E, Wilson, LD, Santos, JH & Nur, M, 2024, 'Chapter 9-Chitosan-based nanomaterials in decontamination of pharmaceutical waste in book "Chitosan-Based Hybrid Nanomaterials"', *In: Chitosan-Based Hybrid Nanomaterials*, 1st edn, pp. 153–180, <https://doi.org/10.1016/B978-0-443-21891-0.00009-3>

Vieira, IRS, de Carvalho, APAd & Conte-Junior, CA 2022, 'Recent advances in biobased and biodegradable polymer nanocomposites, nanoparticles, and natural antioxidants for antibacterial and antioxidant food packaging applications', *Comprehensive reviews in food science and food safety*, vol. 21, no. 4, pp. 3673–3716, <https://doi.org/10.1111/1541-4337.12990>

Wang, S, Zhao, M, Zhou, M, Li, Y, C, Wang, J, Gao, B, Sato, S, Feng, K, Yin, W, Igalavithana, A, D, Oleszczuk, P, Wang, X & Ok, YS 2019, 'Biochar-supported nZVI (nZVI/BC) for contaminant removal from soil and water: A critical review', *Journal of Hazardous Materials*, vol. 373, pp. 820–839, <https://doi.org/10.1016/j.jhazmat.2019.03.080>

Wang, XX, Cheng, F, Wang, XX, Feng, T, Xia, S & Zhang, X 2020, 'Chitosan decoration improves the rapid and long-term antibacterial activities of cinnamaldehyde-loaded liposomes', *International Journal of Biological Macromolecules*, vol. 168, pp. 59–66, <https://doi.org/10.1016/j.ijbiomac.2020.12.003>

Wibowo, A, Jatmiko, A, Ananda, MB, Rachmawati, SA, Ardy, H, Aimon, AH & Iskandar, F 2021, 'Facile fabrication of polyelectrolyte complex nanoparticles based on chitosan – poly-2-acrylamido-2-methylpropane sulfonic acid as a potential drug carrier material', *International Journal of Technology*, vol. 12, no. 3, pp. 561–570, <https://doi.org/10.14716/ijtech.v12i3.4193>

Yang, HC, Wang, WH, Huang, KS & Hon, MH 2010, 'Preparation and application of nanochitosan to finishing treatment with anti-microbial and anti-shrinking properties', *Carbohydrate Polymers*, vol. 79, no. 1, pp. 176–179, <https://doi.org/10.1016/j.carbpol.2009.07.045>

Yang, J, Liang, G, Xiang, T & Situ, W 2021, 'Effect of cross-linking processing on the chemical structure and biocompatibility of a chitosan-based hydrogel', *Food Chemistry*, vol. 354, article 129476, <https://doi.org/10.1016/j.foodchem.2021.129476>

Yuan, G, Chen, X & Li, D 2016, 'Chitosan films and coatings containing essential oils: The antioxidant and antimicrobial activity, and application in food systems', *Food Research International*, vol. 89, pp. 117–128, <https://doi.org/10.1016/j.foodres.2016.10.004>

Zamiah, N, Shaari, K, Rozlee, LH & Faiz Basri, M 2021, 'Synthesis and evaluation of polysulfone/chitosan/polyvinyl alcohol integral composite membranes for the removal of mercury ion', *EVERGREEN: Joint Journal of Novel Carbon Resource Sciences & Green Asia Strategy*, vol. 08, pp. 484–491, <https://doi.org/10.5109/4480733>